

# Exploration of the In Vitro Violacein Synthetic Pathway with Substrate Analogues

Shelby L. Hooe, Meghna Thakur, Guillermo Lasarte-Aragonés, Joyce C. Breger, Scott A. Walper, Igor L. Medintz,\* and Gregory A. Ellis\*



Cite This: *ACS Omega* 2024, 9, 3894–3904



Read Online

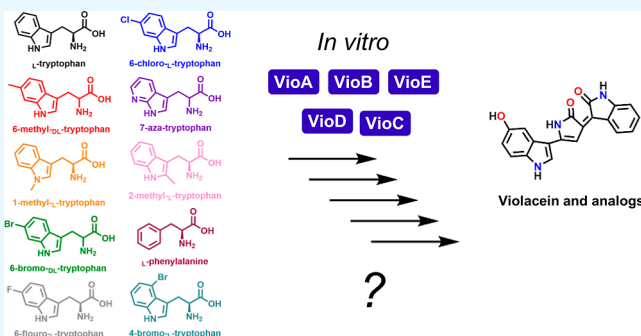
ACCESS |

Metrics & More

Article Recommendations

Supporting Information

**ABSTRACT:** Evolution has gifted enzymes with the ability to synthesize an abundance of small molecules with incredible control over efficiency and selectivity. Central to an enzyme's role is the ability to selectively catalyze reactions in the milieu of chemicals within a cell. However, for chemists it is often desirable to extend the substrate scope of reactions to produce analogue(s) of a desired product and therefore some degree of enzyme promiscuity is often desired. Herein, we examine this dichotomy in the context of the violacein biosynthetic pathway. Importantly, we chose to interrogate this pathway with tryptophan analogues in vitro, to mitigate possible interference from cellular components and endogenous tryptophan. A total of nine tryptophan analogues were screened for by analyzing the substrate promiscuity of the initial enzyme, VioA, and compared to the substrate tryptophan. These results suggested that for VioA, substitutions at either the 2- or 4-position of tryptophan were not viable. The seven analogues that showed successful substrate conversion by VioA were then applied to the five enzyme cascade (VioABEDC) for the production of violacein, where L-tryptophan and 6-fluoro-L-tryptophan were the only substrates which were successfully converted to the corresponding violacein derivative(s). However, many of the other tryptophan analogues did convert to various substituted intermediaries. Overall, our results show substrate promiscuity with the initial enzyme, VioA, but much less for the full pathway. This work demonstrates the complexity involved when attempting to analyze substrate analogues within multienzymatic cascades, where each enzyme involved within the cascade possesses its own inherent promiscuity, which must be compatible with the remaining enzymes in the cascade for successful formation of a desired product.



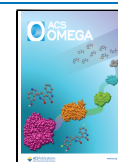
## 1. INTRODUCTION

Synthetic biology in the context of biosynthesis can bring intrinsic benefits to the production of select small molecules versus traditional chemical organic synthesis. Enzymes, the catalysts of these processes, are exquisitely specific, precisely choosing the correct substrate out of the thousands of small molecules in a cell while allowing for regio- and stereospecific control of reactions. This can allow for specific modification of a molecule without protecting groups, as well as one-pot multienzymatic biosyntheses without the need to purify stepwise intermediates.<sup>1–6</sup> Also, creating analogues of product compounds is often desirable, whether to identify structure–activity relationships, to modify the physicochemical properties of a compound, or as a handle for downstream synthetic modifications. In this case, a degree of substrate promiscuity is crucial. However, a complex interplay exists here, particularly in multienzyme cascades where too much promiscuity can lead to off-target byproducts, while too little promiscuity hinders product analogue production.<sup>5,7–9</sup> Different enzymes intrinsically have different substrate promiscuities, leading to different substrate scopes. As has been demonstrated for decades with

traditional chemical synthesis, delineating the substrate scope of a catalyst is crucial for its applicability as this information can inform retrosynthetic schemes for a variety of desired molecules. Additionally, building a portfolio of enzymes which are characterized in terms of substrate promiscuity will be crucial to developing retrobiosynthetic schemes for the still growing field of synthetic biology-driven biosynthesis.<sup>5,10</sup>

Within the field of biosynthesis, two approaches are often used. Cell-based (or “*in vivo*”) biosynthesis relies on engineering chassis strains, often microbial, to produce biosynthetic enzymes and perform reactions within the confines of a cell.<sup>11–13</sup> These systems can either convert growth feedstocks such as glucose to the final product or be fed a specific substrate for the reaction. Cell-free (or “*in vitro*”) biosynthesis

**Received:** October 19, 2023  
**Revised:** December 21, 2023  
**Accepted:** December 26, 2023  
**Published:** January 6, 2024



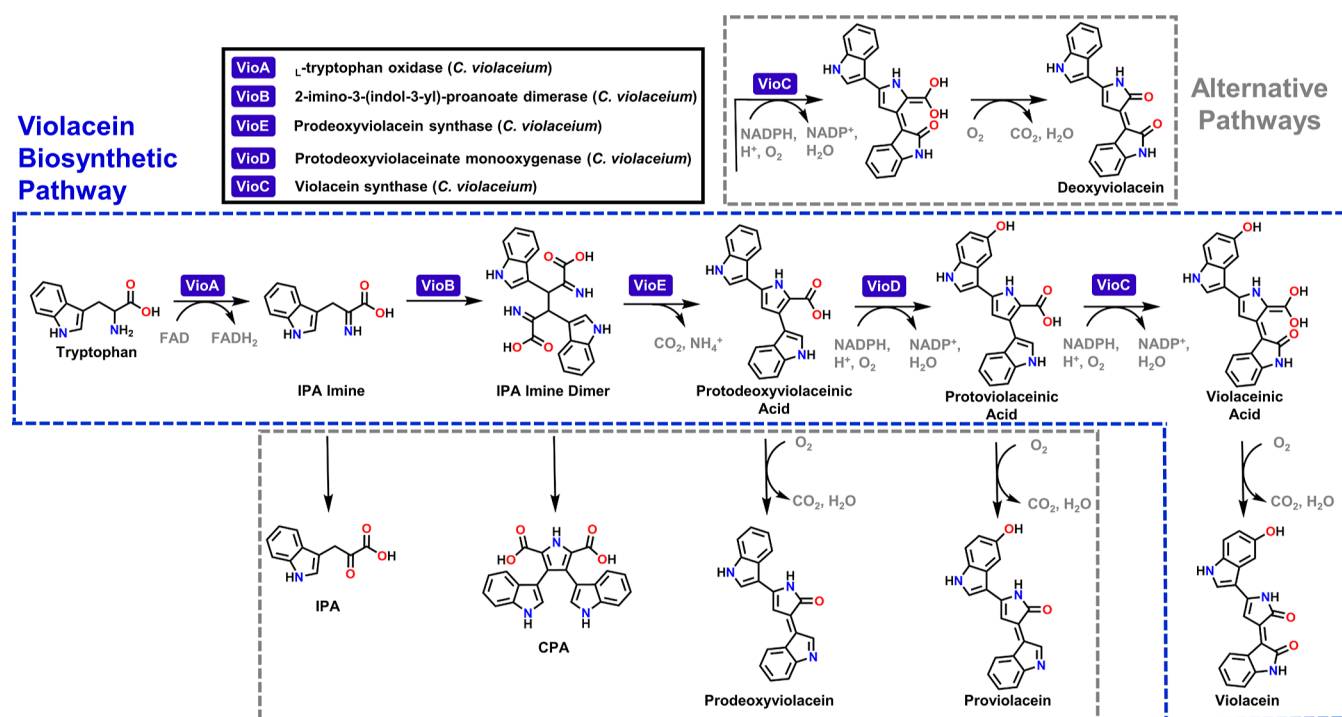


**Figure 1.** Schematic of the five-enzyme biosynthetic pathway to produce violacein, consisting of VioA, VioB, VioE, VioD, and VioC. The alternative pathways illustrate dead-end byproducts that can be formed either enzymatically or nonenzymatically throughout the cascade. Notably, VioC can react with protodeoxyviolaceinic acid in a pathway that ultimately forms the major byproduct deoxyviolacein. IPA imine = indole-3-pyruvic acid imine (2-imino-3-(1*H*-indol-3-yl)propanoic acid); IPA imine dimer = indole-3-pyruvic acid imine dimer (2,5-diimino-3,4-di(1*H*-indol-3-yl)hexanedioic acid); protodeoxyviolaceinic acid = 3,5-di(1*H*-indol-3-yl)-1*H*-pyrrole-2-carboxylic acid; protoviolaceinic acid = 5-(5-hydroxy-1*H*-indol-3-yl)-3-(1*H*-indol-3-yl)-1*H*-pyrrole-2-carboxylic acid; violaceinic acid = (Z)-3-(2-(dihydroxymethylene)-5-(5-hydroxy-1*H*-indol-3-yl)-1,2-dihydro-3*H*-pyrrol-3-ylidene) indolin-2-one; violacein = (Z)-3-(5-(5-hydroxy-1*H*-indol-3-yl)-2-oxo-1,2-dihydro-3*H*-pyrrol-3-ylidene) indolin-2-one; IPA Keto = indole-3-pyruvic acid (3-(1*H*-indol-3-yl)-2-oxopropanoic acid); CPA = chromopyrrolic acid (3,4-di(1*H*-indol-3-yl)-1*H*-pyrrole-2,5-dicarboxylic acid); prodeoxyviolacein = (Z)-5-(1*H*-indol-3-yl)-3-(3*H*-indol-3-ylidene)-1,3-dihydro-2*H*-pyrrol-2-one; proviolacein = (Z)-5-(5-hydroxy-1*H*-indol-3-yl)-3-(3*H*-indol-3-ylidene)-1,3-dihydro-2*H*-pyrrol-2-one; and deoxyviolacein = (Z)-3-(5-(1*H*-indol-3-yl)-2-oxo-1,2-dihydro-3*H*-pyrrol-3-ylidene) indolin-2-one.

relies on enzymes outside of a cellular matrix.<sup>5,14–18</sup> These enzymes can be in a range of purity, from cell-free transcription–translation (TX–TL) protein synthesis lysates that contain the cellular machinery and energetic material to produce enzymes, to crude preparations from cellular expressions with little purification, to the purified enzymes.<sup>19</sup> While cell-based biosynthesis has some inherent benefits, in the context of biosynthesizing product analogues, it can face some significant limitations. Substrate analogues must either be produced within the confines of the cell or must transit the cellular membrane, but if analogues are not naturally encountered by the cell, the cell may lack uptake mechanisms. Furthermore, these analogues are often toxic to cells, killing cells before significant product formation is achieved. For example, modified amino acids can incorporate into and disrupt cellular proteins. Additionally, substrate analogues must compete with endogenous “wild-type” substrates, which can lead to product mixtures and complications with downstream processing. This issue can extend into cell-free biosynthesis if crude lysates are used without purification of enzymes away from endogenous substrates. However, these issues can be mitigated by using the purified enzyme(s) in a minimalist cell-free biosynthetic approach.<sup>5,10,14,16,20–26</sup>

We were therefore interested in examining and characterizing the potential of a cell-free, purified, multienzyme pathway to produce product analogues as one step toward understanding what would eventually be needed for a fuller

retrobiosynthetic capability portfolio. For this examination, we chose the five enzyme biosynthetic pathway for violacein (Figure 1). Violacein is a bis-indole pigmented compound that has demonstrated a variety of bioactivities, including antibacterial, antitumoral, antiviral, trypanocidal, and anti-protozoan, as well as antioxidant activity.<sup>27,28</sup> While an interesting target for a variety of previous synthetic biology studies, this pathway also contains a variety of dead-end byproducts, including chromopyrrolic acid (CPA) which can itself be an intermediate toward the bioactive molecules rebeccamycin and staurosporine, complicating analysis and production of violacein but enhancing potential applicability, see Figure 1.<sup>29–33</sup> Analogues of violacein have previously been produced using cell-based biosynthesis and investigated for bioactivity and downstream chemical modification, notably by the Freemont and Goss laboratories.<sup>34,35</sup> These reports are important for helping to understand violacein activity and make this pathway ideal for additional characterization toward a fuller understanding of its biosynthetic potential. However, the results of these reports indicated mixtures of products due to endogenous tryptophan in this cell-based approach. Herein, we chose to use purified enzymes to obviate this issue.<sup>34,35</sup> We first tested the substrate promiscuity of the initial enzyme, VioA, for an initial series of tryptophan analogues. Next, we down-selected for the most reactive substrate analogues and tested the full VioABEDC pathway. While VioA is fairly promiscuous, the entire pathway was more recalcitrant to

substrate analogues. However, by using a cell-free system, we were able to produce a range of homosubstituted compounds including 6,6'-difluoroviolaecin without interfering tryptophan and thus without mixed products. We anticipate these results will encourage additional use of cell-free multienzyme pathways for analogue production.

## 2. MATERIALS AND METHODS

**2.1. Materials and Chemicals.** All chemicals, buffers, and reagents were from standard vendors, including Millipore (Burlington, MA, USA), SigmaAldrich (St. Louis, MO, USA), ThermoFisher (Waltham, MA, USA), and CarboSynth (now Biosynth, Staad, Switzerland) unless specified.

**2.2. Protein Production.** Genes for VioA, VioB, VioE, VioD, and VioC from *Chromobacterium violaceum* were synthesized by ATUM (DNA TwoPointO, Inc., Newark, CA, USA) and cloned into pET28b (VioA, VioE, VioD, VioC; kanamycin resistant) and pET22b (VioB; ampicillin resistant) expression vectors using the NcoI/XhoI (pET28b) and NdeI/XhoI restriction sites (pET22b), respectively. The expression plasmids were transformed into *Escherichia coli* BL21(DE3) for protein production. Protein production was done similarly as described previously and below.<sup>36–47</sup> Briefly, starter cultures were grown overnight in 5 mL of Luria Broth (LB) with 50  $\mu\text{g/mL}$  kanamycin or 100  $\mu\text{g/mL}$  ampicillin and used to inoculate 500 mL of Terrific Broth (TB, Sigma-Aldrich, USA) with antibiotic in 2 L baffled flasks. Cultures were grown at 37 °C with shaking until the mid log growth phase (supplemented with 1 mM 5-aminolevulinic acid hydrochloride and 40  $\mu\text{M}$  ammonium iron sulfate for pET22b-VioB) and induced with 0.5 mM isopropyl- $\beta$ -D-thiogalactopyranoside (IPTG) then incubated at 25 °C (15 °C for VioB) with shaking overnight. Cells were centrifuged at 4000g, pellets stored at –80 °C, thawed, and resuspended in 30 mL of ice-cold lysis buffer (0.5 $\times$  phosphate-buffered saline (PBS), 0.01% Triton X-100, 1 mM EDTA, and 1 mg/mL lysozyme) followed by three 1 min sonications. The lysate was cleared by centrifugation for 30 min at 8000g, and the soluble fraction was incubated with a 500  $\mu\text{L}$  bed volume equivalent of nitriloacetic acid (Ni-NTA) chromatography resin (GE Healthcare) overnight at 4 °C with constant rotation. Resin was washed in wash buffer (50 mM sodium phosphate, 500 mM NaCl, 10 mM imidazole, pH = 7.5), and protein was eluted with wash buffer containing 300 mM imidazole. The enzymes were further purified by size exclusion chromatography using a BioRad NGC chromatography instrument and an Enrich SEC 650 10  $\times$  300 column (BioRad). Protein fractions containing purified enzymes were pooled and stored at –80 °C in 20% glycerol following snap freezing in a dry ice methanol bath. Core protein sequences can be found in the [Supporting Information](#).

**2.3. Assay for VioA Activity.** The activity of VioA with tryptophan and tryptophan analogues was measured using a previously developed assay.<sup>48</sup> Quinoneimine formation was monitored as a function of time at 505 nm to determine the apparent kinetic parameters of the VioA enzyme. Stock solutions were prepared in 10 mM tris HCl (pH = 9) and consisted of a 10  $\mu\text{M}$  VioA stock, a 500 U/mL horseradish peroxidase (HRP) stock, a 100 mM phenol stock, individual stocks of tryptophan derivatives ranging between 2 and 3 mM, and a 100 mM 4-aminoantipyrene stock. Then, an enzyme containing a solution of 100 nM VioA, 100 U/mL HRP, 10 mM phenol, and 10 mM 4-aminoantipyrene was prepared. The assays were performed in a 40  $\mu\text{L}$  total volume with 20  $\mu\text{L}$  of

the enzyme-containing solution and 20  $\mu\text{L}$  of the tryptophan derivative at variable concentrations (0.025–1.5 mM). The final concentrations for the assays were 50 nM VioA, varied tryptophan derivative (0.025–1.5 mM), 5 mM phenol, 5 mM 4-aminoantipyrene, and 50 U/mL HRP. Reactions were started upon the addition of the tryptophan derivative. Assays were carried out in a 384-well microtiter white transparent bottom plate. The absorbance at 505 nm was followed on a Tecan Spark plate reader utilizing a kinetic program that consisted of shaking the plate for 3 s prior to taking a reading every 26 s. Absorbance values were converted to concentration values utilizing the molar extinction coefficient of the quinoneimine (6400  $\text{M}^{-1} \text{cm}^{-1}$ ). The linear portions of the progress curves were used to calculate the initial rates for each substrate concentration. These were fitted to the Michaelis–Menten (MM) equation using either Excel's solver module or Sigma Plot's enzyme module to determine relevant MM descriptors ( $V_{\text{max}}$ ,  $k_{\text{cat}}$ ,  $K_{\text{M}}$ , and  $k_{\text{cat}}/K_{\text{M}}$ ). All activity measurements were performed on at least three independently assembled replicates.

**2.4. Assay for VioABEDC Activity.** For monitoring production of violacein and violacein analogues, an enzyme stock solution was prepared in 10 mM tris HCl (pH = 9) and consisted of 200 nM VioA, 2000 nM VioB, 2000 nM VioC, 2000 nM VioD, and 2000 nM VioE. Individual stocks of tryptophan derivatives at 2 mM and containing 10 mM nicotinamide adenine dinucleotide phosphate (NADPH) were prepared in 10 mM Tris HCl (pH = 9). The assays were performed in 200  $\mu\text{L}$  total volume with 100  $\mu\text{L}$  of the enzyme stock and 100  $\mu\text{L}$  of the tryptophan derivative with NADPH. The final concentrations for the assays were 100 nM VioA, 1000 nM VioB, 1000 nM VioC, 1000 nM VioD, and 1000 nM VioE with 1 mM of the tryptophan derivative and 5 mM NADPH. Reactions were started upon the addition of the solution containing the tryptophan derivative with NADPH. Reactions were run for 48 h at 30 °C and 60 rpm shaking. Final reaction products were stored at –80 °C until analysis by LC/MS.

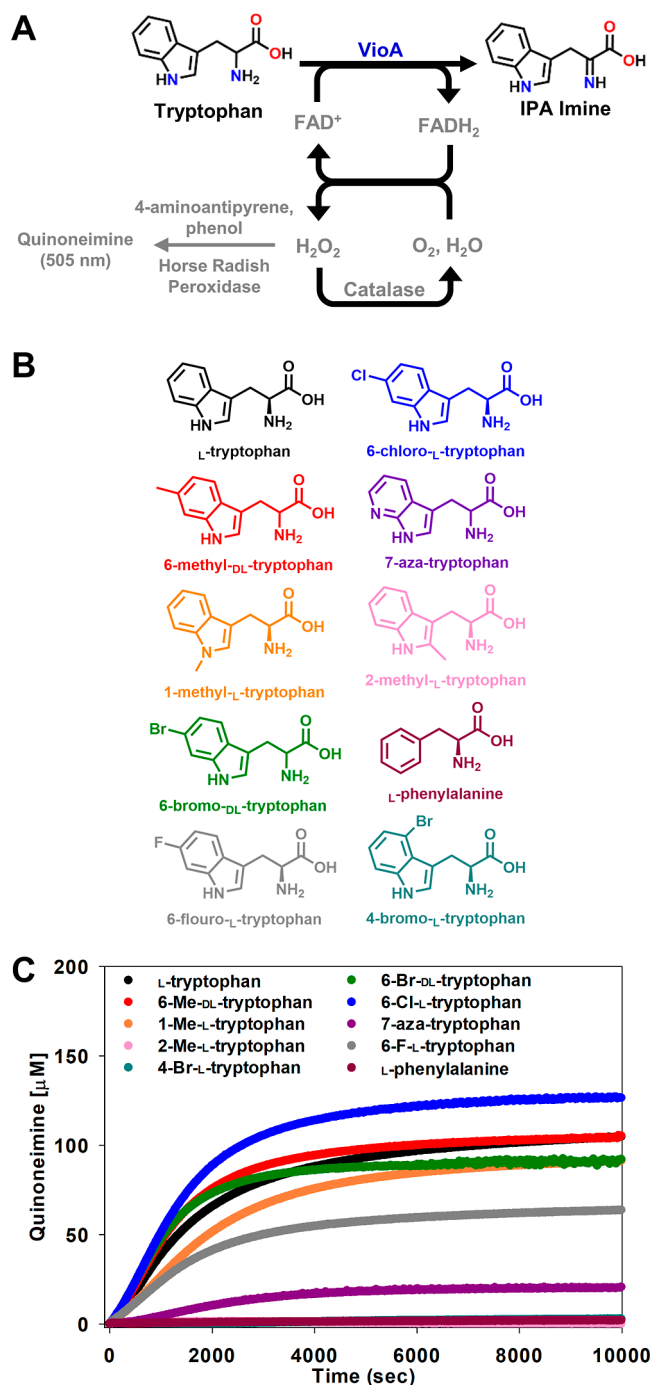
**2.5. LC/MS Analysis.** LC/MS data acquisition was conducted on a Waters system including a Waters Acquity ultra-performance liquid chromatography (UPLC) H-class equipped with an in-line Waters UPLC e $\lambda$  PDA UV–vis spectrophotometric detector and SQ2 mass spectrometer and electrospray ionization source, using an Acquity UPLC BEH C18, 2.1  $\times$  50 mm, 1.7  $\mu\text{m}$ , column (Waters Corp, Milford, MA, USA). Buffer A was 0.1% formic acid in H<sub>2</sub>O and Buffer B was 0.1% formic acid in acetonitrile. The flow rate was 0.4 mL/min, and the column was held at 45 °C. Samples were diluted in acetonitrile to 1:1 and centrifuged at 16,000g for 10 min. Supernatant was injected at 20  $\mu\text{L}$ . The elution gradient was as follows: Initially hold at 10% B for 2 min, linear gradient from 10–90% B over 11 min, hold at 90% for 2.5 min, linear gradient from 90–10% over 0.5 min, then re-equilibrate by holding at 10% B for 2.5 min. Absorbance was measured by means of the photodiode array detected from 200 to 600 nm and 585–750 nm and specifically at 560 nm (for deoxyviolacein) and 575 nm (for violacein). Mass spectrometry was conducted at a 3 kV capillary voltage in the negative mode. Selected ion monitoring was done for selected, expected components (for ions monitored, see [Table S1](#)), and an ESI negative scan was conducted between 100 and 1000  $m/z$ .

### 3. RESULTS

Before testing the five enzyme cascades for the conversion of tryptophan to violacein for a series of tryptophan derivatives, we first examined the ability of the first enzyme in the cascade, VioA, to convert a series of tryptophan derivatives to the corresponding IPA imine product derivative. The activity of the VioA enzyme was screened across nine tryptophan derivatives (plus tryptophan itself) and then the derivatives displaying the best activity for the first step in the cascade were applied to the full five enzyme cascade to identify which substrates were able to form the desired violacein derivatives versus following one of the alternative pathways to form the various dead-end products.

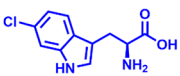
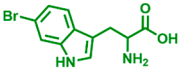
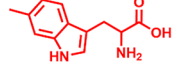
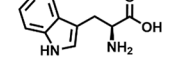
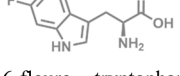
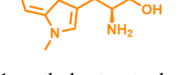
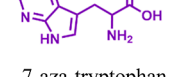
**3.1. VioA Catalyzes Reactions with a Variety of Substrates.** VioA catalyzes the first step in the violacein biosynthetic pathway, converting tryptophan to 2-imino-3-(indol-3-yl)propanoate (IPA imine). Over time, the IPA imine produced can be converted nonenzymatically to the dead-end byproduct indole-3-pyruvic acid (IPA), see Figure 1. During the VioA reaction, the cofactor flavin adenine dinucleotide (FAD) is reduced to FADH<sub>2</sub>; to regenerate the cofactor, O<sub>2</sub> oxidizes FADH<sub>2</sub> back to FAD, forming hydrogen peroxide (H<sub>2</sub>O<sub>2</sub>), see Figure 2A.<sup>29</sup> Therefore, to monitor VioA activity with different analogues, H<sub>2</sub>O<sub>2</sub> was measured by its reaction with 4-aminoantipyrene, phenol, and the catalase enzyme horseradish peroxidase to form a quinoneimine which absorbs spectrophotometrically at 505 nm.<sup>11,48,49</sup> Ten compounds were chosen to test for the reaction with VioA (Figure 2B). These included L-phenylalanine, L-tryptophan, 7-aza-tryptophan, and tryptophan analogues: methyl [positions 1 (L-), 2 (L-), and 6 (DL-)], fluoro (position 6 (L-)), chloro (position 6 (L-)), and bromo (positions 4 (L-) and 6 (DL-)). Other analogues were not tried due to intractable solubility issues. Most of these underwent catalysis by VioA, with the exceptions of phenylalanine, 2-methyl-L-tryptophan, and 4-bromo-L-tryptophan, see Figure 2C.

Variable substrate concentration studies were carried out to determine the Michaelis–Menten parameters ( $V_{max}$ ,  $k_{cat}$ ,  $K_M$ , and  $k_{cat}/K_M$ ) for the VioA enzyme across six of the substrate analogues and compared directly to that of L-tryptophan, the native substrate for VioA (see Table 1, Figures S1–S7, and 3). The catalytic rate ( $k_{cat}$ ) of VioA for the DL-tryptophan derivatives (Figure 3A), 6-methyl-DL-tryptophan (1.15 s<sup>-1</sup>) and 6-bromo-DL-tryptophan (1.2 s<sup>-1</sup>), was greater than the activity of VioA for L-tryptophan (0.75 s<sup>-1</sup>). Additionally, the specificity as shown by enzyme efficiency ( $k_{cat}/K_M$ ) remained greater for 6-methyl-DL-tryptophan ( $6.8 \times 10^{-3} \mu\text{M}^{-1} \times \text{s}^{-1}$ ) and 6-bromo-DL-tryptophan ( $7.8 \times 10^{-3} \mu\text{M}^{-1} \times \text{s}^{-1}$ ) relative to L-tryptophan ( $6.0 \times 10^{-3} \mu\text{M}^{-1} \times \text{s}^{-1}$ ). The  $k_{cat}$  values of VioA for 6-chloro-L-tryptophan (1.2 s<sup>-1</sup>) and 6-fluoro-L-tryptophan (0.94 s<sup>-1</sup>) were also greater than the  $k_{cat}$  value for L-tryptophan (Figure 3B). These results suggest that VioA displays substrate promiscuity for tryptophan derivatives substituted at the six-position for small functional groups (methyl) and electronegative atoms (Br, Cl, and F). For the remaining tryptophan derivatives, 1-methyl-L-tryptophan showed comparable activity to L-tryptophan while 7-aza-tryptophan showed a significant decrease in both  $k_{cat}$  (0.17 s<sup>-1</sup>) and  $K_M$  ( $6.0 \times 10^{-4} \mu\text{M}^{-1} \times \text{s}^{-1}$ ) of VioA relative to L-tryptophan (Figure 3C). Overall, the  $k_{cat}$  value for the different analogues varied between 0.6 and 2.4-fold to that of tryptophan, while  $K_M$  varied between 0.2–1.7-fold, and  $k_{cat}/$



**Figure 2.** Kinetic analysis of VioA activity across different tryptophan substrate derivatives. (A) Schematic of the VioA catalyzed reaction. During catalysis, the cofactor FAD is reduced by VioA to FADH<sub>2</sub>. The FAD cofactor is regenerated by O<sub>2</sub>, which in turn forms H<sub>2</sub>O<sub>2</sub>. H<sub>2</sub>O<sub>2</sub> can be monitored to measure VioA activity with different substrates. (B) Ten substrates (0.4 mM) were tested with VioA, demonstrating moderate substrate promiscuity. The seven permissive substrates are shown in Table 1. (C) Plots of quinoneimine formation versus time comparing VioA activity across the ten different tryptophan derivatives. Conditions for reaction mixtures included 50 nM VioA, 50 U/mL HRP, 5 mM PhOH, and 5 mM aminoantipyrene with approximately 0.5 mM tryptophan derivative in 10 mM Tris buffer at pH = 9. Note that 2-Me-L-tryptophan, 4-Br-L-tryptophan, and L-phenylalanine data overlap near baseline.

**Table 1. Michaelis–Menten Kinetic Parameters for VioA with, from Top to Bottom in Order of Descending  $K_{\text{cat}}/K_{\text{M}}$ : 6-Chloro-L-tryptophan, 6-Bromo-DL-tryptophan, 6-Methyl-DL-tryptophan, L-Tryptophan, 6-Fluoro-L-tryptophan, 1-Methyl-L-tryptophan, and 7-Aza-tryptophan**

Tryptophan Derivative	$V_{\text{max}}$ ( $\mu\text{M} \times \text{s}^{-1}$ )	$K_{\text{M}}$ ( $\mu\text{M}$ )	$k_{\text{cat}}$ ( $\text{s}^{-1}$ )	$k_{\text{cat}}/K_{\text{M}}$ ( $\mu\text{M}^{-1} \times \text{s}^{-1}$ )
 6-chloro-L-tryptophan	0.059 ± 0.007	80 ± 10	1.2 ± 0.14	1.500 (0.004) × 10 <sup>-2</sup>
 6-bromo-DL-tryptophan	0.062 ± 0.005	161 ± 7	1.2 ± 0.11	7.8 (± 0.3) × 10 <sup>-3</sup>
 6-methyl-DL-tryptophan	0.058 ± 0.007	170 ± 20	1.2 ± 0.14	6.80 ± (0.02) × 10 <sup>-3</sup>
 L-tryptophan	0.038 ± 0.003	125 ± 10	0.75 ± 0.07	6.00 (± 0.05) × 10 <sup>-3</sup>
 6-fluoro-L-tryptophan	0.047 ± 0.002	182 ± 6	0.94 ± 0.04	5.2 (± 0.4) × 10 <sup>-3</sup>
 1-methyl-L-tryptophan	0.038 ± 0.002	300 ± 10	0.77 ± 0.04	2.6 (± 0.2) × 10 <sup>-3</sup>
 7-aza-tryptophan	0.0085 ± 0.0005	300 ± 15	0.17 ± 0.01	6.0 (± 0.6) × 10 <sup>-4</sup>

$K_{\text{M}}$  varied between 0.4–10.7-fold. The identification of 6-fluoro-L-tryptophan as a VioA substrate coincides with data reported by Lai et al. and Wilkenson et al.,<sup>34,35</sup> and of 1-methyl-L-tryptophan and 7-aza-tryptophan with data reported by Fuller et al.<sup>48</sup> Together, the data compiled by ourselves and these other groups allows for an emerging picture of what is and is not tolerated by VioA, see Table S2. Note that many of these tryptophan analogues show some toxicity to strains of *E. coli*, a common biosynthesis organism. While toxicity does not preclude some use of these analogues by VioA in cells, as shown by Lai and Wilkenson, it would presumably hinder large-scale production using these analogues (see Discussion).<sup>34,35</sup>

**3.2. Biosynthesis Using the Full Violacein Pathway, VioABEDC.** Inspired by the ability of VioA to catalyze reactions with the majority of the analogues tested, we next turned to synthesis of violacein and violacein analogues using the full VioABEDC pathway. As previously mentioned, the full pathway can result in several dead-end byproducts, including the major byproduct deoxyviolacein, as well as the violacein product itself, see Figure 1. We performed the reactions using pairwise combinations of each of the 7 substrates for 28 total reactions, see Table 2, and compared the results to a control without enzymes (see Figures S8–S12). While VioA was promiscuous to these seven substrates, in our hands the entire pathway was only permissive to L-tryptophan and 6-fluoro-L-

tryptophan, forming violacein, the single 6-fluoro-violacein analogue, and the dual 6-fluoro-violacein analogue. A fairly conservative approach was used to denote production of violacein or analogues thereof (see discussion below). It is important to note that our analysis is qualitative and not quantitative. This is due to the fact that many of the products do not exist for LC/MS standardization methods, and our interests were focused on identifying the viable substrate scope of the five enzyme cascades.

In regard to the main byproduct deoxyviolacein, analysis was complicated by the fact that proviolacein has the same mass. Therefore, while mass spectral peaks were seen for many of these combinations, it cannot be said which compound they represent. However, we note that proviolacein is produced through VioABED, and deoxyviolacein is produced through VioABEC; therefore, regardless of the product, when a peak is identified, there is an indication that the substrates were tolerated by at least VioABE.

For those reactions in which a single substrate was used, LC/MS analysis was conducted for several intermediates and dead-end byproducts in the pathway, see Figure 4. The results indicate that while the violacein analogue was not produced by most reactions, several intermediates were. Of particular note, all substrates except for 7-aza-tryptophan formed chromopyrrolic acid, a key intermediate toward production of rebeccamycin and staurosporine.

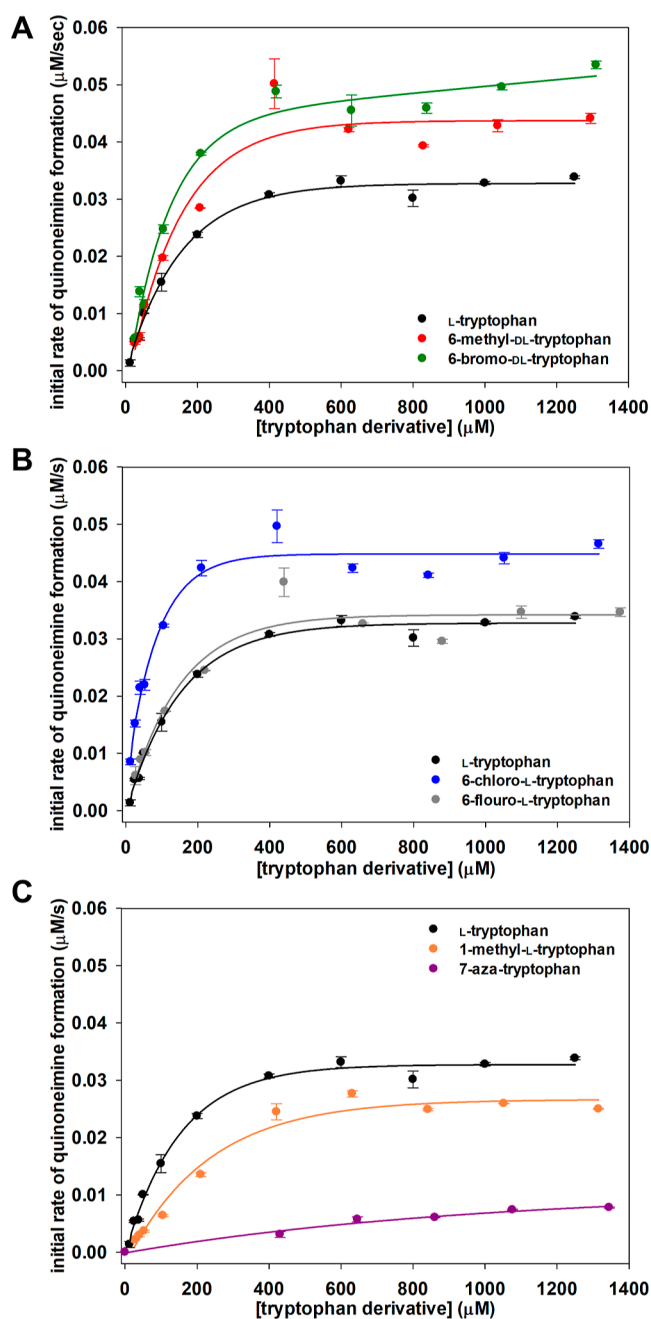


**Figure 3.** Michaelis–Menten plots for VioA activity generated by monitoring the absorbance of quinoneimine, which reports on  $\text{H}_2\text{O}_2$  production. (A) Michaelis–Menten analysis of L-tryptophan, 6-methyl-DL-tryptophan, and 6-bromo-DL-tryptophan. (B) Michaelis–Menten analysis of L-tryptophan, 6-chloro-L-tryptophan, and 6-fluoro-L-tryptophan. (C) Michaelis–Menten analysis of L-tryptophan, 1-methyl-L-tryptophan, and 7-aza-tryptophan.

#### 4. DISCUSSION

Several of the tryptophan analogues used here and in other publications have been shown to be quite toxic to wild-type *E. coli*, a common bioproduction microorganism.<sup>50–52</sup> This could be due to incorporation into and disruption of endogenous proteins, inhibition of enzymes, or binding to proteins that normally bind tryptophan or through other mechanisms. This toxicity does not preclude the use of these analogues in cell-based biosynthesis as shown by the cell-based production of violacein analogues by other groups.<sup>34,35</sup> However, it is

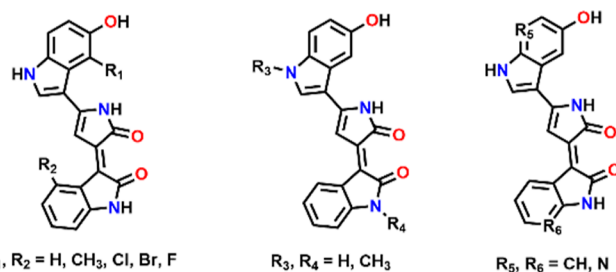
anticipated that toxicity would preclude the use of high substrate analogue concentrations, which in turn could hinder overall yield in scale-up reactions. The addition of tryptophan in addition to tryptophan analogues may help alleviate this toxicity, but results in mixtures of violacein, tryptophan-analogue violacein, and dual analogue violacein as shown by others.<sup>34,35</sup> This adds complexity to downstream processing and may still not result in much increased yield. The same issue would presumably be seen in any cell-free TX/TL system as these systems require tryptophan for endogenous protein production in that system during any assay. Therefore, this system seems ideally suited for examination of analogue production using a purified, multienzyme cascade.

**4.1. VioA Substrate Tolerance.** The activity of the first biosynthetic enzyme, VioA, can be relatively easily monitored spectrophotometrically by measuring the production of  $\text{H}_2\text{O}_2$ . We demonstrated that VioA was permissive to many substrate analogues, adding to the substrate repertoire of VioA as determined by others.<sup>34,35,48</sup> In our hands, the 2-position and the 4-position were particularly recalcitrant to activity. This could be due to a number of factors, including steric exclusion of the VioA active site or modified electronic efforts of tryptophan due to this substitution. Interestingly, previous reports indicate that all other amino acids are not tolerated by VioA, with the exception of slight activity with phenylalanine (1.8% relative to tryptophan; we saw little-to-no activity herein, see Figure 2C).<sup>48,53</sup> This has been hypothesized to help avoid toxic  $\text{H}_2\text{O}_2$  production in the cell.<sup>48</sup>

**4.2. Substrate Tolerance of the Multienzymatic Violacein Cascade.** The production of violacein by the entire VioABEDC pathway was monitored by LC/UV–vis/MS. Violacein has a distinct absorbance at 575 nm whereas the byproduct deoxyviolacein absorbs at 560 nm, and each has a unique mass versus the other. While this absorbance is hard to differentiate by batch spectrophotometry, the two can be separated by LC.

To examine the substrate scope of the violacein pathway using our selected analogues, 28 reactions were conducted with either single substrates or pairwise combinations. The detection of violacein or violacein analogues was determined by both UV–vis and MS. Mass spectral chromatographic peaks for violacein/violacein analogues were detected for many of the reaction combinations; however, many of these peaks had overlapping retention times with chromopyrrolic acid and did not show corresponding UV–vis peaks at 575 nm. While violacein analogues may have a different UV–vis absorbance than violacein, we anticipate the absorbance to be close or overlapping, and suspect the more likely result that chromopyrrolic acid is fragmenting during mass spectral analysis, giving the corresponding (false) violacein analogue *m/z* peak. Therefore, these reactions were designated as not producing the violacein analogue at a yield within our limit of detection, or “NO\*” in Table 2. We do note that some analogues produced violaceinic acid but not the nonenzymatically made violacein; this could be due to a variety of reasons, including detection limits for our method (UV, MS, or both) or some other unknown aspect of these violaceinic acid analogues that minimizes conversion to violacein. Regarding deoxyviolacein, this compound has an identical mass to proviolacein, and while these compounds do absorb at different wavelengths, the absorbance is relatively close and may shift with analogues; therefore, we chose the conservative approach to denote the peaks as deoxyviolacein/proviolacein.

**Table 2. Analysis of Violaecine Analogue and Deoxyviolaecine/Proviolaecine Analogue Production Using Combinations of Tryptophan Analogues<sup>a</sup>**



#	R <sub>1</sub>	R <sub>2</sub>	R <sub>3</sub>	R <sub>4</sub>	R <sub>5</sub>	R <sub>6</sub>	abbreviation	analogue observed	
								violaecine	deoxyviolaecine/proviolaecine
1	H	H	H	H	CH	H	Trp-Trp	yes	yes
2	H	CH <sub>3</sub>	H	H	CH	H	Trp-6Me	no*	yes
3	H	H	H	CH <sub>3</sub>	CH	H	Trp-1Me	no*	yes
4	H	Br	H	H	CH	H	Trp-6Br	no*	yes
5	H	Cl	H	H	CH	H	Trp-6Cl	no*	no
6	H	H	H	H	CH	N	Trp-7aza	no*	yes
7	H	F	H	H	CH	H	Trp-6F	yes	yes
8	CH <sub>3</sub>	CH <sub>3</sub>	H	H	CH	H	6Me-6Me	no*	yes
9	CH <sub>3</sub>	H	H	CH <sub>3</sub>	CH	H	6Me-1Me	no*	yes
10	CH <sub>3</sub>	Br	H	H	CH	H	6Me-6Br	no*	yes
11	CH <sub>3</sub>	Cl	H	H	CH	H	6Me-6Cl	no*	yes
12	CH <sub>3</sub>	H	H	H	CH	N	6Me-7aza	no*	yes
13	CH <sub>3</sub>	F	H	H	CH	H	6Me-6F	no**	yes
14	H	H	CH <sub>3</sub>	CH <sub>3</sub>	CH	H	1Me-1Me	no*	yes
15	H	Br	CH <sub>3</sub>	H	CH	H	1Me-6Br	no*	yes
16	H	Cl	CH <sub>3</sub>	H	CH	H	1Me-6Cl	no*	yes
17	H	H	CH <sub>3</sub>	H	CH	N	1Me-7aza	no*	yes
18	H	F	CH <sub>3</sub>	H	CH	H	1Me-6F	no*	yes
19	Br	Br	H	H	CH	H	6Br-6Br	no*	no
20	Br	Cl	H	H	CH	H	6Br-6Cl	no*	no
21	Br	H	H	H	CH	N	6Br-7aza	no*	no
22	BR	F	H	H	CH	H	6Br-6F	no*	no
23	Cl	Cl	H	H	CH	H	6Cl-6Cl	no*	yes
24	Cl	H	H	H	CH	N	6Cl-7aza	no	no
25	Cl	F	H	H	CH	H	6Cl-6F	no*	yes
26	H	H	H	H	N	N	7aza-7aza	no*	yes
27	H	F	H	H	N	H	7aza-6F	no*	no
28	F	F	H	H	CH	H	6F-6F	yes	yes

<sup>a</sup>Structures of violaecine analogues are depicted at the top. Note that deoxyviolaecine and proviolaecine have the same mass and therefore cannot be distinguished. \* indicates that while a violaecine mass peak was identified, no corresponding UV-vis peak was and therefore the peak was likely in-source fragmentation of chromopyrrolic acid. \*\* indicates there was a mass peak with a corresponding UV-vis peak, but the peaks were too far separated, and likely the UV-vis peak corresponds to the dual 6-fluoro violaecine analogue. Abbreviations: Trp = tryptophan. 1Me = 1-methyl-L-tryptophan. 6Me = 6-methyl-DL-tryptophan. 6Br = 6-bromo-DL-tryptophan. 6Cl = 6-chloro-L-tryptophan. 7aza = 7-aza-tryptophan. 6F = 6-fluoro-L-tryptophan.

Many of the reactions produced deoxyviolaecine/proviolaecine peaks, indicating tolerance of VioABE and either VioC or VioD to these analogues; see Table 2. Deoxyviolaecine has been shown to have bioactivity itself, indicating a potential use to any deoxyviolaecine analogues formed.<sup>27,54</sup>

We were particularly interested in single substrate analogues as these would be uniquely easier to form in the cell-free system than in the cell-based system. Therefore, we also analyzed these reactions for other intermediates and dead-end byproducts in the pathway, see Figure 1 (chromoviridans and deoxychromoviridans were excluded for simplicity). Many of these were identified, although we acknowledge that these identifications are putative as commercial standards are not available for most for comparison. However, given the

aggregated results, this indicates the general tolerance of most of the pathway. In particular, most of the tryptophan analogues formed the corresponding chromopyrrolic acid analogue, which is an intermediate toward the production of the apoptotic compound rebeccamycin and the kinase inhibitor staurosporine.<sup>55–57</sup> Our initial survey results reported here, that some of the violaecine downstream enzymes VioB, VioE, VioC, and VioD seem permissive to various substrates, indicate that future kinetic analyses of these enzymes with various analogues may be warranted. However, we anticipate these studies to be complicated due to the instability of the intermediates of this pathway (i.e., intermediates form dead-end byproducts) and are beyond the current scope.

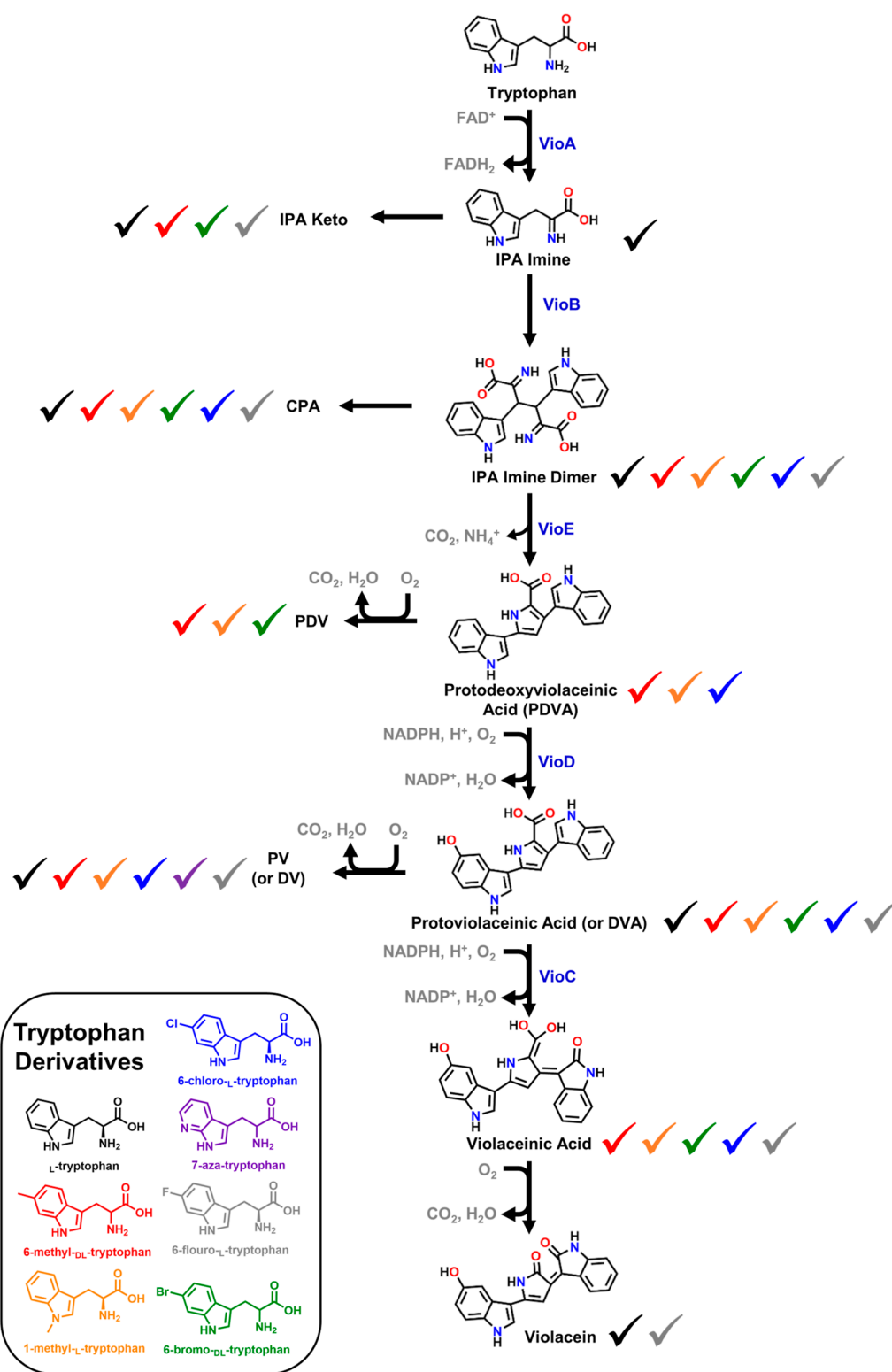


**Figure 4.** Results from analysis of intermediate and analogue product formed and identified via LC/MS using solely one tryptophan analogue at a time. Note that deoxyviolacein and proviolacein have the same mass while PVA and DVA also have the same mass; therefore, these compounds cannot be distinguished from each other. For 6-Me-DL-tryptophan, 1-Me-L-tryptophan, 6-Br-DL-tryptophan, 6-Cl-L-tryptophan, and 7-aza-tryptophan a violacein mass peak was identified, but no corresponding UV-vis peak was identified; therefore, the peak was likely in-source fragmentation of chromopyrrolic acid. The color of the check marks adjacent to the structures correspond to the products identified from the different tryptophan derivatives color coded inside the black box. CPA = chromopyrrolic acid. PVA/DVA = protoviolaceinic acid/deoxyviolaceinic acid, which have the same mass. PDVA = protodeoxyviolaceinic acid. PV/DV = proviolacein/deoxyviolacein, which have the same mass. PDV = protodeoxyviolacein. IPA = indole-3-pyruvic acid.



**4.3. Production of Violacein Analogues from 6-Fluoro-L-tryptophan.** The substrate 6-fluoro-L-tryptophan produced both the single fluoro violacein analogue and the dual fluoro violacein analogue. We hypothesize that the 6-fluoro substitution was well tolerated due to its small size relative to the methyl and other halogen substitutions. Lai et al. demonstrated that the single 5-bromo violacein analogue could undergo subsequent chemical synthesis using Suzuki–Miyaura cross-coupling.<sup>34</sup> Fluorine tends to be more recalcitrant than bromine to this chemistry but can be used for other cross-coupling reactions, such as Grignard-type reactions (although this may require protecting groups).<sup>58</sup> Fluorine is a relatively common substitution to many chemicals in regard to changing their physicochemical properties due to the high strength and polarization of the C–F bond and could be useful in-and-of itself for violacein.<sup>59</sup> Fluorine-18 is also used for positron emission topography, indicating potential usefulness of this substitution for positron emission topography studies using violacein.<sup>60</sup> Finally, we are encouraged that our proof-of-concept study was able to produce a dual fluoro violacein analogue without any interfering tryptophan in the reaction as would be the case for a cell-based synthesis.

## 5. CONCLUSIONS

In conclusion, multiple enzymes in the violacein pathway appear tolerant to tryptophan analogues. This demonstration could encourage future enzyme engineering efforts that may enhance this tolerance. We anticipate that future studies such as the ones reported here will not only facilitate the biosynthesis of product analogues but also add to the repertoire of knowledge regarding the substrate scope of enzymatic biosynthesis, allowing for better prediction for retrobiosynthesis.

## ■ ASSOCIATED CONTENT

### SI Supporting Information

The Supporting Information is available free of charge at <https://pubs.acs.org/doi/10.1021/acsomega.3c08233>.

Protein sequences, supplementary assay data, and supplementary LC/MS data (PDF)

## ■ AUTHOR INFORMATION

### Corresponding Authors

**Igor L. Medintz** – *Center for Bio/Molecular Science and Engineering Code 6900, U.S. Naval Research Laboratory, Washington, D.C. 20375, United States*; [orcid.org/0000-0002-8902-4687](https://orcid.org/0000-0002-8902-4687); Email: [igor.medintz@nrl.navy.mil](mailto:igor.medintz@nrl.navy.mil)

**Gregory A. Ellis** – *Center for Bio/Molecular Science and Engineering Code 6900, U.S. Naval Research Laboratory, Washington, D.C. 20375, United States*; [orcid.org/0000-0001-5559-3809](https://orcid.org/0000-0001-5559-3809); Email: [gregory.ellis@nrl.navy.mil](mailto:gregory.ellis@nrl.navy.mil)

### Authors

**Shelby L. Hooe** – *National Research Council, Washington, D.C. 20001, United States*; *Center for Bio/Molecular Science and Engineering Code 6900, U.S. Naval Research Laboratory, Washington, D.C. 20375, United States*

**Meghna Thakur** – *Center for Bio/Molecular Science and Engineering Code 6900, U.S. Naval Research Laboratory, Washington, D.C. 20375, United States*; *College of Science, George Mason University, Fairfax, Virginia 22030, United States*

**Guillermo Lasarte-Aragonés** – *Center for Bio/Molecular Science and Engineering Code 6900, U.S. Naval Research Laboratory, Washington, D.C. 20375, United States*; *College of Science, George Mason University, Fairfax, Virginia 22030, United States*; Present Address: Affordable and Sustainable Sample Preparation (AS2P) research group, Departamento de Química Analítica, Instituto Químico para la Energía y el Medioambiente IQUEMA, Campus de Rabanales, Universidad de Córdoba, Edificio Marie Curie, Córdoba E-14071, Spain; [orcid.org/0000-0003-3502-9367](https://orcid.org/0000-0003-3502-9367)

**Joyce C. Breger** – *Center for Bio/Molecular Science and Engineering Code 6900, U.S. Naval Research Laboratory, Washington, D.C. 20375, United States*

**Scott A. Walper** – *Center for Bio/Molecular Science and Engineering Code 6900, U.S. Naval Research Laboratory, Washington, D.C. 20375, United States*; Present Address: US Office of Naval Research, 86 Blenheim Crescent, Ruislip, Middlesex HA4 7GB, UK.

Complete contact information is available at: <https://pubs.acs.org/10.1021/acsomega.3c08233>

## Author Contributions

S.L.H. and M.T. contributed equally and share first authorship. All authors provided initial concepts, study/experimental design, and/or project management. S.L.H. and M.T. prepared enzymes. S.L.H., M.T., G.L., J.C.B., and G.A.E. undertook experimental performance, analysis, and interpretation. All authors contributed to writing/reading/editing and approved the final manuscript.

## Notes

The authors declare no competing financial interest.

## ■ ACKNOWLEDGMENTS

The authors acknowledge the Office of Naval Research (ONR), the U.S. Naval Research Laboratory (NRL), and the NRL Nanoscience Institute for funding support. S.L.H. acknowledges a National Research Council (NRC) Fellowship through NRL. I.L.M. and G.A.E. acknowledge the National Institute of Food and Agriculture, U.S. Department of Agriculture, under Award #2020-67021-31254 and the Strategic Environmental Research Development Program (SERDP), under Award # WP21-1073 New Start Project (W74RDV03497375). The funders had no role in study design, data collection and analysis, or preparation of the manuscript.

## ■ REFERENCES

- (1) Biz, A.; Proulx, S.; Xu, Z.; Siddartha, K.; Mulet Indrayanti, A.; Mahadevan, R. Systems biology based metabolic engineering for non-natural chemicals. *Biotechnol. Adv.* **2019**, *37* (6), 107379.
- (2) Clomburg, J. M.; Crumbley, A. M.; Gonzalez, R. Industrial biomanufacturing: The future of chemical production. *Science* **2017**, *355* (6320), aag0804.
- (3) El Karoui, M.; Hoyos-Flight, M.; Fletcher, L. Future Trends in Synthetic Biology-A Report. *Front. Bioeng. Biotechnol.* **2019**, *7*, 175.
- (4) Ellis, G. A.; Klein, W. P.; Lasarte-Aragonés, G.; Thakur, M.; Walper, S. A.; Medintz, I. L. Artificial Multienzyme Scaffolds: Pursuing in Vitro Substrate Channeling with an Overview of Current Progress. *ACS Catal.* **2019**, *9* (12), 10812–10869.
- (5) Hooe, S. L.; Ellis, G. A.; Medintz, I. L. Alternative design strategies to help build the enzymatic retrosynthesis toolbox. *RSC Chem. Biol.* **2022**, *3* (11), 1301–1313.

- (6) National Research Council. *Industrialization of Biology: A Roadmap to Accelerate the Advanced Manufacturing of Chemicals*; The National Academies Press: Washington, DC, 2015; p 167.
- (7) Cornish-Bowden, A. *Fundamentals of Enzyme Kinetics*, 4th ed.; Elsevier: Weinheim, Germany, 2012.
- (8) Turner, N. J. Directed evolution drives the next generation of biocatalysts. *Nat. Chem. Biol.* **2009**, *5* (8), 567–573.
- (9) Zeymer, C.; Hilvert, D. Directed Evolution of Protein Catalysts. *Annu. Rev. Biochem.* **2018**, *87*, 131–157.
- (10) Lin, G.-M.; Warden-Rothman, R.; Voigt, C. A. Retrosynthetic design of metabolic pathways to chemicals not found in nature. *Curr. Opin. Syst. Biol.* **2019**, *14*, 82–107.
- (11) Keasling, J. D. Manufacturing molecules through metabolic engineering. *Science* **2010**, *330* (6009), 1355–1358.
- (12) Lee, S. Y.; Kim, H. U. Systems strategies for developing industrial microbial strains. *Nat. Biotechnol.* **2015**, *33* (10), 1061–1072.
- (13) Lee, S. Y.; Kim, H. U.; Chae, T. U.; Cho, J. S.; Kim, J. W.; Shin, J. H.; Kim, D. I.; Ko, Y.-S.; Jang, W. D.; Jang, Y.-S. A comprehensive metabolic map for production of bio-based chemicals. *Nat. Catal.* **2019**, *2* (1), 18–33.
- (14) Bowie, J. U.; Sherkhanov, S.; Korman, T. P.; Valliere, M. A.; Opgenorth, P. H.; Liu, H. Synthetic Biochemistry: The Bio-inspired Cell-Free Approach to Commodity Chemical Production. *Trends Biotechnol.* **2020**, *38* (7), 766–778.
- (15) Ellis, G. A.; Díaz, S. A.; Medintz, I. L. Enhancing enzymatic performance with nanoparticle immobilization: improved analytical and control capability for synthetic biochemistry. *Curr. Opin. Biotechnol.* **2021**, *71*, 77–90.
- (16) Garamella, J.; Marshall, R.; Rustad, M.; Noireaux, V. The All E. coli TX-TL Toolbox 2.0: A Platform for Cell-Free Synthetic Biology. *ACS Synth. Biol.* **2016**, *5* (4), 344–355.
- (17) Garenne, D.; Noireaux, V. Cell-free transcription-translation: engineering biology from the nanometer to the millimeter scale. *Curr. Opin. Biotechnol.* **2019**, *58*, 19–27.
- (18) Opgenorth, P. H.; Korman, T. P.; Bowie, J. U. A synthetic biochemistry molecular purge valve module that maintains redox balance. *Nat. Commun.* **2014**, *5*, 4113.
- (19) Thakur, M.; Breger, J. C.; Susumu, K.; Oh, E.; Spangler, J. R.; Medintz, I. L.; Walper, S. A.; Ellis, G. A. Self-assembled nanoparticle-enzyme aggregates enhance functional protein production in pure transcription-translation systems. *PLoS One* **2022**, *17* (3), No. e0265274.
- (20) Ertek, B.; Akgül, C.; Dilgin, Y. Photoelectrochemical glucose biosensor based on a dehydrogenase enzyme and NAD<sup>+</sup>/NADH redox couple using a quantum dot modified pencil graphite electrode. *RSC Adv.* **2016**, *6* (24), 20058–20066.
- (21) Jiang, L.; Zhao, J.; Lian, J.; Xu, Z. Cell-free protein synthesis enabled rapid prototyping for metabolic engineering and synthetic biology. *Synth. Syst. Biotechnol.* **2018**, *3* (2), 90–96.
- (22) Lu, Y. Cell-free synthetic biology: Engineering in an open world. *Synth. Syst. Biotechnol.* **2017**, *2* (1), 23–27.
- (23) Meyer, C.; Nakamura, Y.; Rasor, B. J.; Karim, A. S.; Jewett, M. C.; Tan, C. Analysis of the Innovation Trend in Cell-Free Synthetic Biology. *Life* **2021**, *11* (6), 551.
- (24) Noireaux, V.; Liu, A. P. The New Age of Cell-Free Biology. *Annu. Rev. Biomed. Eng.* **2020**, *22*, 51–77.
- (25) Rabe, K. S.; Muller, J.; Skoupi, M.; Niemeyer, C. M. Cascades in Compartments: En Route to Machine-Assisted Biotechnology. *Angew. Chem., Int. Ed. Engl.* **2017**, *56* (44), 13574–13589.
- (26) Smanski, M. J.; Zhou, H.; Claesen, J.; Shen, B.; Fischbach, M. A.; Voigt, C. A. Synthetic biology to access and expand nature's chemical diversity. *Nat. Rev. Microbiol.* **2016**, *14* (3), 135–149.
- (27) Choi, S. Y.; Yoon, K. H.; Lee, J. I.; Mitchell, R. J. Violacein: Properties and Production of a Versatile Bacterial Pigment. *BioMed Res. Int.* **2015**, *2015*, 465056.
- (28) Fang, M. Y.; Zhang, C.; Yang, S.; Cui, J. Y.; Jiang, P. X.; Lou, K.; Wachi, M.; Xing, X. H. High crude violacein production from glucose by *Escherichia coli* engineered with interactive control of tryptophan pathway and violacein biosynthetic pathway. *Microb. Cell Fact.* **2015**, *14*, 8.
- (29) Balibar, C. J.; Walsh, C. T. In vitro biosynthesis of violacein from L-tryptophan by the enzymes VioA-E from *Chromobacterium violaceum*. *Biochemistry* **2006**, *45* (51), 15444–15457.
- (30) Ellis, G. A.; Tschirhart, T.; Spangler, J.; Walper, S. A.; Medintz, I. L.; Vora, G. J. Exploiting the Feedstock Flexibility of the Emergent Synthetic Biology Chassis *Vibrio natriegens* for Engineered Natural Product Production. *Mar. Drugs* **2019**, *17* (12), 679.
- (31) Hoshino, T. Violacein and related tryptophan metabolites produced by *Chromobacterium violaceum*: biosynthetic mechanism and pathway for construction of violacein core. *Appl. Microbiol. Biotechnol.* **2011**, *91* (6), 1463–1475.
- (32) Sanchez, C.; Brana, A. F.; Mendez, C.; Salas, J. A. Reevaluation of the violacein biosynthetic pathway and its relationship to indolocarbazole biosynthesis. *Chembiochem* **2006**, *7* (8), 1231–1240.
- (33) Wang, Y.; Heermann, R.; Jung, K. CipA and CipB as Scaffolds To Organize Proteins into Crystalline Inclusions. *ACS Synth. Biol.* **2017**, *6* (5), 826–836.
- (34) Lai, H. E.; Obled, A. M. C.; Chee, S. M.; Morgan, R. M.; Lynch, R.; Sharma, S. V.; Moore, S. J.; Polizzi, K. M.; Goss, R. J. M.; Freemont, P. S. GenoChemetic Strategy for Derivatization of the Violacein Natural Product Scaffold. *ACS Chem. Biol.* **2021**, *16* (11), 2116–2123.
- (35) Wilkinson, M. D.; Lai, H. E.; Freemont, P. S.; Baum, J. A. Biosynthetic Platform for Antimalarial Drug Discovery. *Antimicrob. Agents Chemother.* **2020**, *64* (5), No. e02129.
- (36) Breger, J. C.; Ancona, M. G.; Walper, S. A.; Oh, E.; Susumu, K.; Stewart, M. H.; Deschamps, J. R.; Medintz, I. L. Understanding How Nanoparticle Attachment Enhances Phosphotriesterase Kinetic Efficiency. *ACS Nano* **2015**, *9* (8), 8491–8503.
- (37) Breger, J. C.; Oh, E.; Susumu, K.; Klein, W. P.; Walper, S. A.; Ancona, M. G.; Medintz, I. L. Nanoparticle Size Influences Localized Enzymatic Enhancement—A Case Study with Phosphotriesterase. *Bioconjugate Chem.* **2019**, *30* (7), 2060–2074.
- (38) Breger, J. C.; Vranish, J. N.; Oh, E.; Stewart, M. H.; Susumu, K.; Lasarte-Aragónés, G.; Ellis, G. A.; Walper, S. A.; Díaz, S. A.; Hooe, S. L.; Klein, W. P.; Thakur, M.; Ancona, M. G.; Medintz, I. L. Self assembling nanoparticle enzyme clusters provide access to substrate channeling in multienzymatic cascades. *Nat. Commun.* **2023**, *14* (1), 1757.
- (39) Breger, J. C.; Walper, S. A.; Oh, E.; Susumu, K.; Stewart, M. H.; Deschamps, J. R.; Medintz, I. L. Quantum dot display enhances activity of a phosphotriesterase trimer. *Chem. Commun.* **2015**, *51* (29), 6403–6406.
- (40) Brown Iii, C. W.; Oh, E.; Hastman, D. A.; Walper, S. A.; Susumu, K.; Stewart, M. H.; Deschamps, J. R.; Medintz, I. L. Kinetic enhancement of the diffusion-limited enzyme beta-galactosidase when displayed with quantum dots. *RSC Adv.* **2015**, *5* (113), 93089–93094.
- (41) Claussen, J. C.; Malanoski, A.; Breger, J. C.; Oh, E.; Walper, S. A.; Susumu, K.; Goswami, R.; Deschamps, J. R.; Medintz, I. L. Probing the Enzymatic Activity of Alkaline Phosphatase within Quantum Dot Bioconjugates. *J. Phys. Chem. C* **2015**, *119* (4), 2208–2221.
- (42) Díaz, S. A.; Choo, P.; Oh, E.; Susumu, K.; Klein, W. P.; Walper, S. A.; Hastman, D. A.; Odom, T. W.; Medintz, I. L. Gold Nanoparticle Templating Increases the Catalytic Rate of an Amylase, Maltase, and Glucokinase Multienzyme Cascade through Substrate Channeling Independent of Surface Curvature. *ACS Catal.* **2021**, *11* (2), 627–638.
- (43) Dwyer, C. L.; Díaz, S. A.; Walper, S. A.; Samanta, A.; Susumu, K.; Oh, E.; Buckhout-White, S.; Medintz, I. L. Chemoenzymatic Sensitization of DNA Photonic Wires Mediated through Quantum Dot Energy Transfer Relays. *Chem. Mater.* **2015**, *27* (19), 6490–6494.
- (44) Hondred, J. A.; Breger, J. C.; Garland, N. T.; Oh, E.; Susumu, K.; Walper, S. A.; Medintz, I. L.; Claussen, J. C. Enhanced enzymatic activity from phosphotriesterase trimer gold nanoparticle bioconjugates for pesticide detection. *Analyst* **2017**, *142* (17), 3261–3271.

- (45) Medintz, I. L.; Goldman, E. R.; Lassman, M. E.; Mauro, J. M. A fluorescence resonance energy transfer sensor based on maltose binding protein. *Bioconjugate Chem.* **2003**, *14* (5), 909–918.
- (46) Medintz, I. L.; Matthew Mauro, J. Use of a Cyanine Dye as a Reporter Probe in Reagentless Maltose Sensors Based on E. coli Maltose Binding Protein. *Anal. Lett.* **2004**, *37* (2), 191–202.
- (47) Samanta, A.; Walper, S. A.; Susumu, K.; Dwyer, C. L.; Medintz, I. L. An enzymatically-sensitized sequential and concentric energy transfer relay self-assembled around semiconductor quantum dots. *Nanoscale* **2015**, *7* (17), 7603–7614.
- (48) Fuller, J. J.; Ropke, R.; Krausze, J.; Rennhack, K. E.; Daniel, N. P.; Blankenfeldt, W.; Schulz, S.; Jahn, D.; Moser, J. Biosynthesis of Violacein, Structure and Function of L-Tryptophan Oxidase VioA from *Chromobacterium violaceum*. *J. Biol. Chem.* **2016**, *291* (38), 20068–20084.
- (49) Saito, Y.; Mifune, M.; Nakashima, S.; Odo, J.; Tanaka, Y.; Chikuma, M.; Tanaka, H. Determination of Hydrogen Peroxide with Phenol and 4-Aminoantipyrine by the Use of a Resin Modified with Manganese-Tetrakis(sulfophenyl)porphine. *Anal. Sci.* **1987**, *3* (2), 171–174.
- (50) Browne, D. R.; Kenyon, G. L.; Hegeman, G. D. Incorporation of monofluorotryptophans into protein during the growth of *Escherichia coli*. *Biochem. Biophys. Res. Commun.* **1970**, *39* (1), 13–19.
- (51) Kuhn, J. Detection of antimetabolite activity: effects and transport of tryptophan analogs in *Escherichia coli*. *Antimicrob. Agents Chemother.* **1977**, *12* (3), 322–327.
- (52) Kuhn, J. C.; Pabst, M. J.; Somerville, R. L. Mutant strains of *Escherichia coli* K-12 exhibiting enhanced sensitivity to 5-methyl-tryptophan. *J. Bacteriol.* **1972**, *112* (1), 93–101.
- (53) Kameya, M.; Onaka, H.; Asano, Y. Selective tryptophan determination using tryptophan oxidases involved in bis-indole antibiotic biosynthesis. *Anal. Biochem.* **2013**, *438* (2), 124–132.
- (54) Jiang, P. X.; Wang, H. S.; Xiao, S.; Fang, M. Y.; Zhang, R. P.; He, S. Y.; Lou, K.; Xing, X. H. Pathway redesign for deoxyviolacein biosynthesis in *Citrobacter freundii* and characterization of this pigment. *Appl. Microbiol. Biotechnol.* **2012**, *94* (6), 1521–1532.
- (55) Howard-Jones, A. R.; Walsh, C. T. Staurosporine and rebeccamycin aglycones are assembled by the oxidative action of StaP, StaC, and RebC on chromopyrrolic acid. *J. Am. Chem. Soc.* **2006**, *128* (37), 12289–12298.
- (56) National Center for Biotechnology Information. *PubChem Compound Summary for CID 73110, Rebeccamycin*; Pubchem, 2023.
- (57) National Center for Biotechnology Information. *PubChem Compound Summary for CID 44259, Staurosporine*; Pubchem, 2023.
- (58) Muller, V.; Ghorai, D.; Capdevila, L.; Messinis, A. M.; Ribas, X.; Ackermann, L. C-F Activation for C(sp<sup>2</sup>)-C(sp<sup>3</sup>) Cross-Coupling by a Secondary Phosphine Oxide (SPO)-Nickel Complex. *Org. Lett.* **2020**, *22* (17), 7034–7040.
- (59) Agostini, F.; Sinn, L.; Petras, D.; Schipp, C. J.; Kubyshkin, V.; Berger, A. A.; Dorrestein, P. C.; Rappsilber, J.; Budisa, N.; Koks, B. Multiomics Analysis Provides Insight into the Laboratory Evolution of *Escherichia coli* toward the Metabolic Usage of Fluorinated Indoles. *ACS Cent. Sci.* **2021**, *7* (1), 81–92.
- (60) Alauddin, M. M. Positron emission tomography (PET) imaging with (18)F-based radiotracers. *Am. J. Nucl. Med. Mol. Imaging* **2012**, *2* (1), 55–76.